Journal of The Korean Astronomical Society
44: 125 ∼ 134, 2011 August

http://dx.doi.org/10.5303/JKAS.2011.44.4.125
ISSN:1225-4614
http://jkas.kas.org

MEDIUM RESOLUTION SPECTRAL LIBRARY OF LATE-TYPE STELLAR TEMPLATES IN NEAR-INFRARED BAND

Huynh Anh Nguyen Le[1], Wonseok Kang[1], Soojong Pak[1], Myungshin Im[2], Jeong-Eun Lee[1], Luis C. Ho[3], Tae-Soo Pyo[4], and Daniel T. Jaffe[1,5]

[1] School of Space Research, Kyung Hee University, 1 Seocheon-dong, Giheung-gu, Yongin, Gyeonggi-do 446-701, Korea
E-mail : huynhanh7@khu.ac.kr, wskang@khu.ac.kr, soojong@khu.ac.kr, and jeongeun.lee@khu.ac.kr
[2] Department of Physics and Astronomy, Seoul National University, Seoul, 151-747, Korea
E-mail : mim@astro.snu.ac.kr
[3] The Observatories of the Carnegie Institution for Science, 813 Santa Barbara Street, Pasadena, CA 91101, USA
E-mail : lho@obs.carnegiescience.edu
[4] Subaru Telescope, National Astronomical Observatory of Japan, 650 North Aohoku Place, Hilo, HI 96720, USA
E-mail : pyo@subaru.naoj.org
[5] Department of Astronomy, University of Texas at Austin, Austin, TX 78712, USA
E-mail : dtj@astro.as.utexas.edu
(Received January 07, 2011; Revised June 30, 2011; Accepted July 25, 2011)

ABSTRACT

We present medium resolution (R = 5000 − 6000) spectra in the near-infrared band, 1.4 − 1.8 μm, for template stars in G, K, and M types observed by the echelle spectrometer, IRCS, at the SUBARU 8.2 m telescope. The identification of lines is based on the spectra of Arcturus (K2 III) in the literature. We measured the equivalent of widths and compared our results to those of Meyer et al. (1998). We conclude that our spectral resolution (R = 6000) data can investigate more accurately the properties of lines in stellar spectra. The library of the template stellar spectra in ASCII format are available for download on the World Wide Web.

Key words : stars: late-type — methods: observational — methods: data analysis

1. INTRODUCTION

The near-infrared (near-IR) band of the stellar spectra have been poorly studied, even though they are useful windows to examine natures of various astronomical sources, e.g., the physical and chemical processes taking place in stellar atmosphere (Heras et al. 2002). In addition, such stellar templates are potentially useful for studying the relation between active galactic nuclei (AGNs) and their host galaxy properties, providing reference lines for measuring the velocity dispersions (e.g., Riffel et al. 2008).

Current efforts in compiling libraries of template stars in G, K, and M types have been performed at low to moderate spectral resolution (R ≤ 3000; Wallace & Hinkle 1997; Meyer et al. 1998; Rayner et al. 2009; Pickles et al. 1998). Recently, new instruments on the 8-m class telescopes provide medium and high resolution spectra of R = 5000 − 20000. It is now important to provide stellar spectral library that matches the resolution of these newer instruments.

In this paper, we present the near-IR H-band spectra (1.4 − 1.8 μm) of G, K and M type stars. The spectra are taken with moderate resolution (R of = 5000 − 10000), improving the spectral resolution of the previous works, or broadening the wavelength coverage. Section 2 presents the samples, the observations, and the data reduction processes. In Section 3, the results and discussions of the spectra are given. We calculate and analyze equivalent widths (EWs) of the line and suggest a way to estimate the effective temperature for giant stars from EWs. Summary and future works are presented in Section 4.

2. OBSERVATIONS AND DATA REDUCTIONS

2.1 Sample

We select the bright template stars ($H < 5$ mag) in spectral classes (G, K, and M) in the luminosity class of III. The giant stars are expected to be the dominant stellar populations of bulges of AGN host galaxies. Table 1 shows the spectral types and near-IR magnitudes of our samples.

2.2 Observation

The observations were performed at the SUBARU 8.2 m telescope using the IRCS (Tokunaga et al . 1998b; Kobayashi et al. 2000) on 2003 Feb 11 UT

Corresponding Author: W. Kang

Table 1.
Sample selection

Object Name	Spectral Type	J[a] (mag)	H[a] (mag)	K[a] (mag)
HD39357	A0V	4.789±0.286	4.734±0.264	4.487±0.016
HD105388	A0V	7.343±0.021	7.390±0.024	7.359±0.027
HD64938	G8III	4.892±0.244	4.192±0.234	4.049±0.276
HD148287	G8III	4.635±0.212	4.013±0.194	3.957±0.202
HD55184	K0III	4.204±0.328	3.473±0.276	3.437±0.298
HD155500	K0III	4.377±0.272	3.760±0.228	3.706±0.194
HD52071	K2III	5.041±0.232	4.295±0.198	...
HD146084	K2III	4.614±0.250	3.823±0.200	3.741±0.230
HD122675	K2III	4.316±0.302	3.538±0.222	3.244±0.344
HD154610	K5III	3.943±0.268	3.165±0.200	2.896±0.252
HD76010	M0III	4.266±0.268	3.332±0.198	3.095±0.278
NSV3729	M0III	2.055±0.278	1.216±0.190	1.144±0.200

[a] Magnitudes in SIMBAD (http://simbad.u-strasbg.fr/).
Reference: 2003yCat2246... (Cutri)

Table 2.
Observation log

Date (UT)	Object Name	Echelle Setting	Slit Width (arcsec)	R	Total Exposure (sec)	Seeing (arcsec)	Airmass
2003 Feb 11	HD39357	$H+$	0.3	10000	4×20	0.80	1.06
...	HD122675	$H+$	0.3	10000	4×12	0.80	1.33
...	NSV3729	$H+$	0.3	10000	4×10	0.80	1.06
2004 Apr 3	HD105388	$H-$	0.6	5000	4×20	0.07	1.08
	...	$H+$	0.6	5000	4×20	0.07	1.08
...	HD55184	$H+$	0.6	5000	4×6	0.30	1.04
...	...	$H-$	0.6	5000	4×6	0.30	1.04
...	HD64938	$H-$	0.6	5000	4×10	0.30	1.04
...	...	$H+$	0.6	5000	4×10	0.30	1.04
...	HD148287	$H-$	0.6	5000	4×10	0.14	1.08
...	...	$H+$	0.6	5000	4×10	0.14	1.08
...	HD155500	$H-$	0.6	5000	4×10	0.14	1.06
...	...	$H+$	0.6	5000	4×10	0.14	1.06
2004 Apr 4	HD52071	$H-$	0.6	5000	4×6	0.40	1.04
...	...	$H+$	0.6	5000	4×6	0.40	1.04
...	HD76010	$H-$	0.6	5000	4×5	0.40	1.01
...	...	$H+$	0.6	5000	4×5	0.40	1.01
...	HD154610	$H-$	0.6	5000	4×5	0.36	1.30
...	...	$H+$	0.6	5000	4×5	0.36	1.30
...	HD146084	$H+$	0.6	5000	4×10	0.36	1.30
...	...	$H-$	0.6	5000	4×10	0.36	1.30

and 2004 April 3 and 4 UT. Table 2 shows logs of the observations.

In the 2003 observations, we observed two template stars, K2 III (HD122675) and M0 III (NSV3729). We also took an A0 V standard star (HD39357) to correct the telluric absorption lines in the target spectra. The weather conditions were clear and the natural seeing was 0.8 arcsec. The slit width was 0.3 arcsec whose spectral resolving power is 10000. The position angle of the slit was 0 deg. The echelle settings of the observations were in $H+$ band covering the wavelength range of $1.47 - 1.82$ μm. The simple frame exposure time was about 10 sec for each target.

The standard A0 V star and the template stars were observed in the nod-on-slit (*ABBA*) mode in which the target is taken in two positions, A and B, along the slit.

In 2004, we observed eight template stars, G8 III (HD64938 and HD148287), K0 III (HD55184 and HD155500), K2 III (HD52071 and HD146084), K5 III (HD154610), and M0 III (HD76010). The standard star A0 V (HD105388) was also observed. The slit width was 0.6 arcsec whose spectral resolving power is 5000. The echelle was set to cover the whole H-bands in the standard $H-$ and $H+$ settings. Other instrument settings and observing modes were the same as in 2003.

2.3 Data Reductions

Data reduction processes were done by *IRAF* * followed by the method described in Pyo (2002). In addition, Python language was used in some tasks to derive the final spectra of targets. Fig. 1 shows the data reduction sequences.

We first made a combined dark frame. All the dark-subtracted data images were corrected for cosmic rays and bad pixels. We used a bad pixel mask (BadPixel070502.fits) provided by the SUBARU IRCS team. Cosmic rays were identified using the detection threshold of 1000 in *COSMICRAYS* within a 5×5 box area. Flat-field correction was done by using normalized flat field images. We also derived the order extraction solutions for echellogram images. This task will be explained in the reduction processes of the standard star. We used telluric OH emission lines as references for wavelength calibrations and geometric distortions (Rousselot et al. 2000).

The telluric absorption lines in the stellar spectra is corrected by dividing for the standard star A0 V spectra. The spectra of standard star needs to be corrected for the Bracket lines from the stellar atmosphere. To do this step, we fitted a Gaussian profile to a Bracket absorption line using the *SPLOT* task in *IRAF*. Fig. 2 shows the spectrum of A0 V star with Bracket lines before and after correction. The *CONTINUUM* task is used for normalization of the flux (see Fig. 3).

In the case of the slit width of 0.6 arcsec, the spectral resolution of the point source depends on the seeing size, while the unresolved spectral lines of the extended sources like sky background or galaxies show a box-shaped profile. In order to match the spectral resolutions of the telluric OH emissions, the standard

* *IRAF* (Image Reduction and Analysis Facility) is distributed by the National Optical Astronomy Observatories (NOAO) which is operated by the Association of Universities for Research in Astronomy (AURA), Inc. under cooperative agreement with the National Science Foundation.

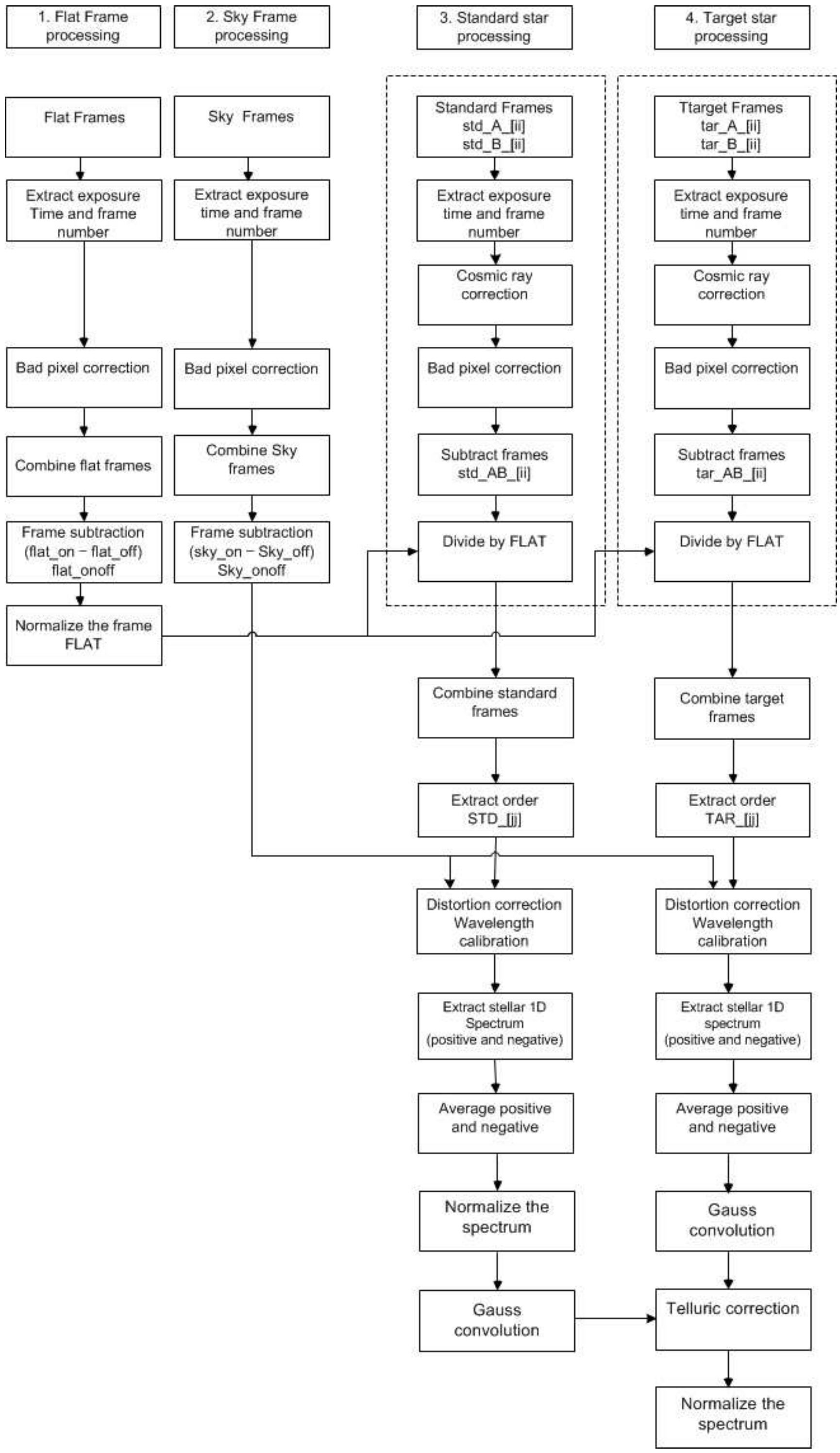

Fig. 1.— Data Reduction Processes.

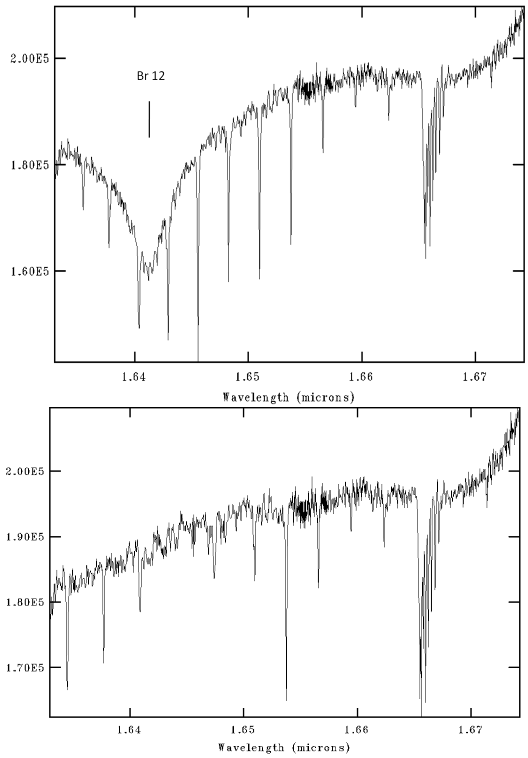

Fig. 2.— Sample spectra of HD39357 (A0 V). The top panel shows a Bracket line Br12 at 1.6412 μm, and the bottom panel after Br12 correction processes.

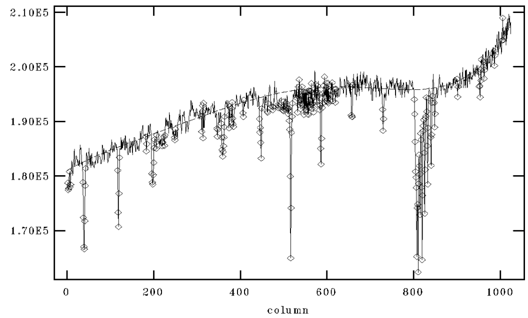

Fig. 3.— Sample spectrum of HD39357 (A0 V) during continuum task in IRAF.

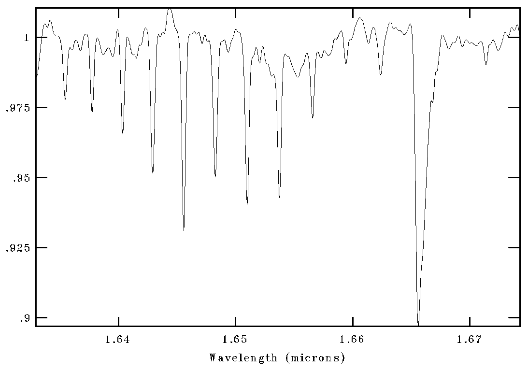

Fig. 4.— Sample spectrum of HD39357 (A0 V) after GAUSS task in IRAF.

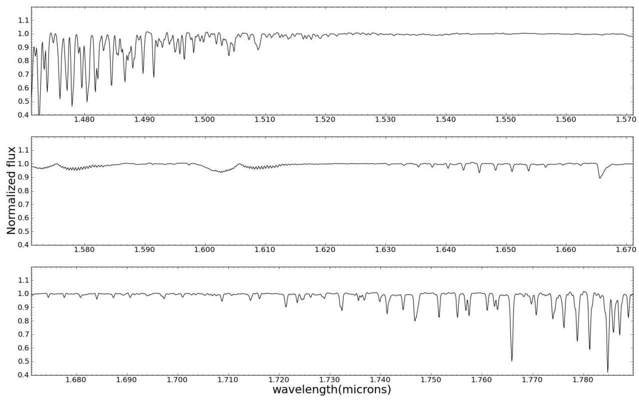

Fig. 5.— Spectra of A0 V standard stars, from combining HD39357 and HD10538.

stars, and the template stars, we convolved the spectra by using the *GAUSS* process with sigma = 2.942 to make FWHM = 8 pixels (1 pixel = 3.94×10^{-5} μm). After the spectral convolution process, the resulting resolution is between 5000 and 6000. Fig. 4 shows the spectra after the *GAUSS* process.

Finally, after getting the final spectrum of each aperture from *IRAF*, we made a laced average spectrum for A0 V standard star using Python language. In this program, we concatenated all the aperture spectra to one spectrum in H-band, and made average spectrum of $H+$ and $H-$ settings. Fig. 5 shows the final spectrum of A0 V standard star whose wavelength has a step of 0.0001μm. Note that the signal-to-noise ratio is very high (S/N $\approx$ 100).

The data reduction processes of template stars are the same as those of the standard stars, except the extraction of 1D spectrum for the distortion corrections, and Bracket line corrections. By dividing for the A0 V star spectra, we corrected the telluric absorption lines in the template spectra. Finally, we used the *CONTINUUM* task to normalize the flux in the spectra.

The Doppler shift in the stellar spectra due to Earth′s motions was corrected by using heliocentric velocity which is obtained from the *RVCORRECT* task. We also corrected the Doppler shift of the proper motions by checking a prominent stellar absorption line.

3. RESULTS AND DISCUSSIONS

3.1 Template Spectra

Fig. 6 shows reduced template spectra in this work and spectrum of Arcturus (K2 III) from Hinkle & Wallace et al.(1995) which is convoluted by using the *GAUSS* task to convert the spectral resolution from R = 100000 to R = 6000. We can see that most of the identified features are very similar to each other. Table 3 lists the identified lines in our data.

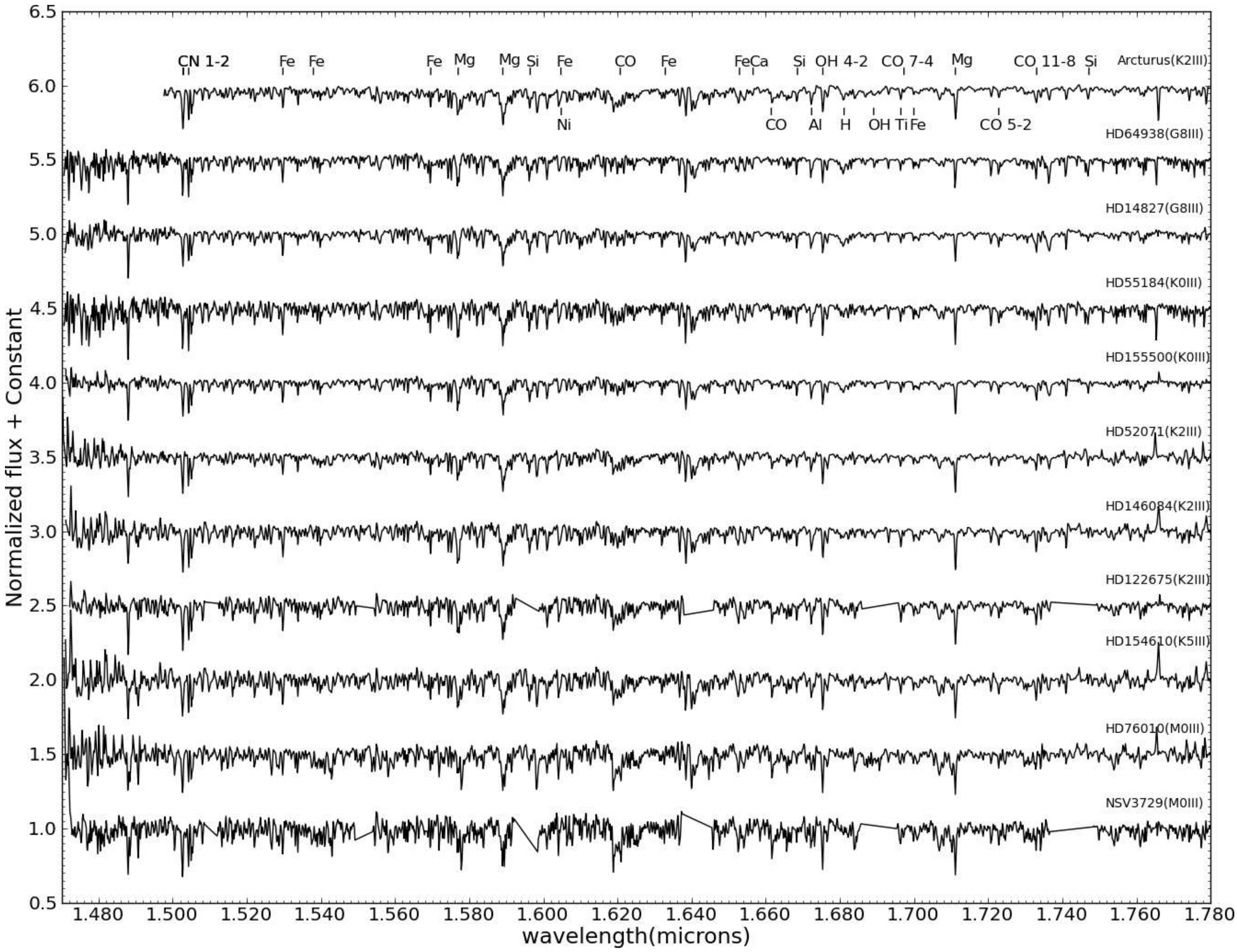

Fig. 6.— Spectra of the template stars in G-K-M types. All of the identified features in the spectra are indicated at the Arcturus (K2 III) spectrum.

Note that some normalized flux values of the spectra are above unity. Even though they are not noise of the spectra, they are just regarded as noise during the *CONTINUUM* task. In addition, the emission lines at $\lambda < 1.48$ μm and $\lambda > 1.76$ μm are not real lines since these regions are on the boundary of H-band where the telluric absorption lines are too deep to be subtracted.

Our obtained H-band spectra cover the the broad absorption $\nu = 3 - 6$ ^{12}CO band head at 1.62073 μm. This broad absorption feature is very useful for kinematic extraction. This absorption feature has a robust comparison between stellar spectra and host galaxy spectra (McConnell et al. 2011). We plan to use this CO band head for measuring the velocity dispersion in the central region of QSO host galaxies. Fig. 7 shows the broad absorption $\nu = 3 - 6$ ^{12}CO band head at 1.62073 μm in our spectra of G8-M0 stars, including Arcturus (K2 III).

3.2 Equivalent Widths

From the identified lines of our spectra based on the referent lines of Arcturus (K2 III) spectra (Hinkle & Wallace et al. 1995), we measured the equivalent widths (EWs) of 9 features which are prominent in the spectra on A-M spectral types (Meyer et al. 1998, hereafter M98). The formula for estimating the EWs and the variance, σ_{EW}, are given by

$$EW = \int_{\lambda_{min}}^{\lambda_{max}} \{1 - F(\lambda)\}\, d\lambda \qquad (1)$$

$$\sigma_{EW} = \Delta\lambda \sqrt{< {\sigma_F}^2 >} \qquad (2)$$

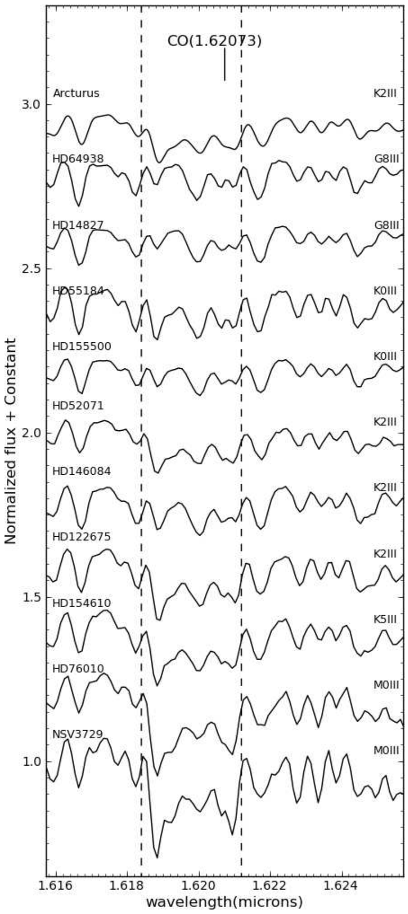

Fig. 7.— CO (1.62073 μm) line for Arcturus and G-K-M type stars. The dash lines show the ranges of EW measurements. CO (1.62073 μm) is potential for measuring the velocity dispersion in the central region of QSO host galaxies.

Table 3.
Identified lines in the reduced template star spectra

Line[a]	Wavelengths (μm)	Features	EW measurement
CN 1-2	1.50284	Strong	No
CN 1-2	1.50430	Strong	No
Fe	1.52973	Strong	No
Fe	1.53795	Weak	No
Fe	1.56961	Strong	No
Mg	1.57701	Strong	Yes
Mg	1.58905	Strong	No
Si	1.59644	Strong	Yes
Fe	1.60471	Strong	No
Ni	1.60481	Weak	No
CO	1.62073	Broad	Yes
Fe	1.63289	Weak	No
Fe	1.65290	Strong	No
Ca	1.65656	Weak	No
CO	1.66147	Broad	Yes
Si	1.66853	Strong	Yes
Al	1.67235	Strong	Yes
OH 4-2	1.67538	Broad	No
H	1.68111	Broad	Yes
OH	1.68909	Narrow	Yes
Ti	1.69644	Strong	No
CO 7-4	1.69727	Narrow	No
Fe	1.69994	Weak	No
Mg	1.71113	Strong	Yes
CO 5-2	1.72284	Weak	No
CO 11-8	1.73307	Strong	No
Si	1.74717	Weak	No

[a] Identified lines from Hinkle & Wallace (1995).

Where $F(\lambda)$ is the normalized flux, and σ_F is the root mean square value (RMS). Table 4 shows the results of EWs in units of wave number (cm^{-1}). The effective temperature in the table are taken from Tokunaga (1998a).

In order to investigate the effect of spectral resolution, we convolved the high resolution spectra (R = 100000) of Arcturus (Hinkle & Walllace 1995) to make the resolutions correspond to our spectra of R = 6000 and to the M98 spectra of R = 3000. Fig. 8 and 9 show two Mg lines (1.57701 μm and 1.71113 μm) of Arcturus with different spectral resolution. Table 3.3 shows the results of EW measurements from the Arcturus spectrum of each resolution in wave number units (cm^{-1}). Assuming that σ_F is 0.1 in the Arcturus spectrum, we calculated the errors of EWs from the formula (2). The Mg (1.57701 μm) line is severely contaminated with other lines, so the EW results of R = 6000 and R = 3000 are different from that of R = 100000. And the EW of Mg (1.71113 μm) line for the spectrum of R = 6000 is very similar to that of R = 100000, while that of R = 3000 shows large difference from the EW result of R = 100000. From a comparison with EWs in spectra with a different resolution, we can assert that our EW results in the spectrum with R = 6000 are more accurate than those of M98 with R = 3000.

3.3 Equivalent Width vs. Temperature

We present 4 specific lines which show the different relation between effective temperature and EWs. Fig. 10 shows the lines of Si (1.59644 μm), Si (1.66853 μm), Mg (1.57701 μm) and Mg (1.71113 μm) in our spectra of G8-M0 stars, including Arcturus (K2 III). The results of EWs and effective temperatures are presented in Fig. 11 and 12. From these figures, we can see that our EW results are smaller than those of M98. This discrepancy of EWs might come from different spectral resolution between our spectra and that of M98.

In M98, the authors might have calculated the EWs with wider range than ours. In this case, the EW results might be contaminated with nearby lines. As shown in Fig. 11, the EW trend of Si (1.59644 μm) line in our result is different from that in M98. It is likely

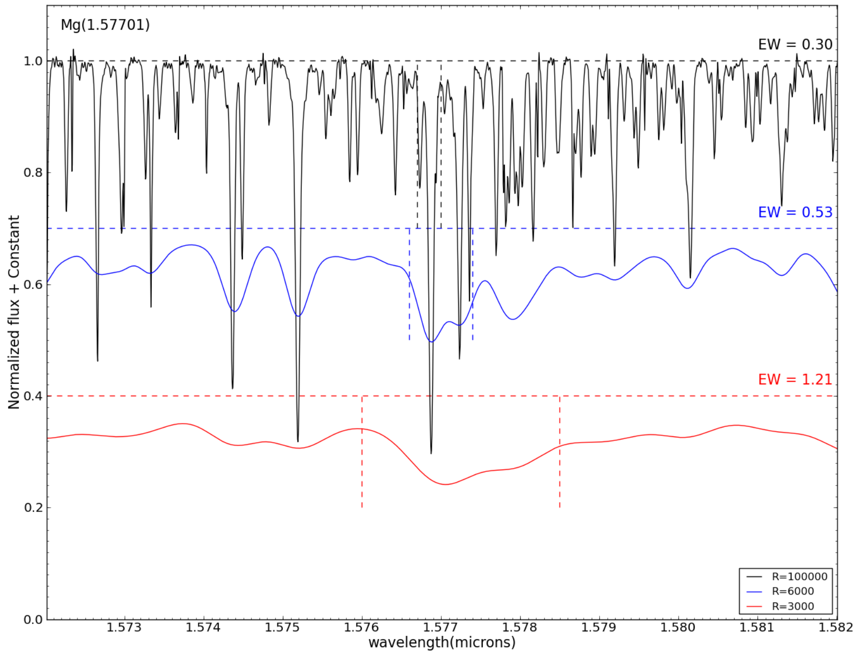

Fig. 8.— Mg (1.57701 μm) spectra in Arcturus (Hinkle & Wallace 1995) with resolutions of R = 100000 (top), R = 6000 (middle), and R = 3000 (bottom). The horizontal dark, blue and red dash lines show the continua. The vertical dark (1.5767 μm-1.5770 μm), blue (1.5766 μm-1.5774 μm), and red (1.5760 μm-1.5785 μm) dash lines show the width ranges (λ_{min}, λ_{max}) which use for calculating the EWs. More lines can be seen in the spectrum of R = 6000 compare with that of R = 3000. Because the contaminated lines can not be separated of R = 6000 and R = 3000, the EW values are larger than those of R = 100000.

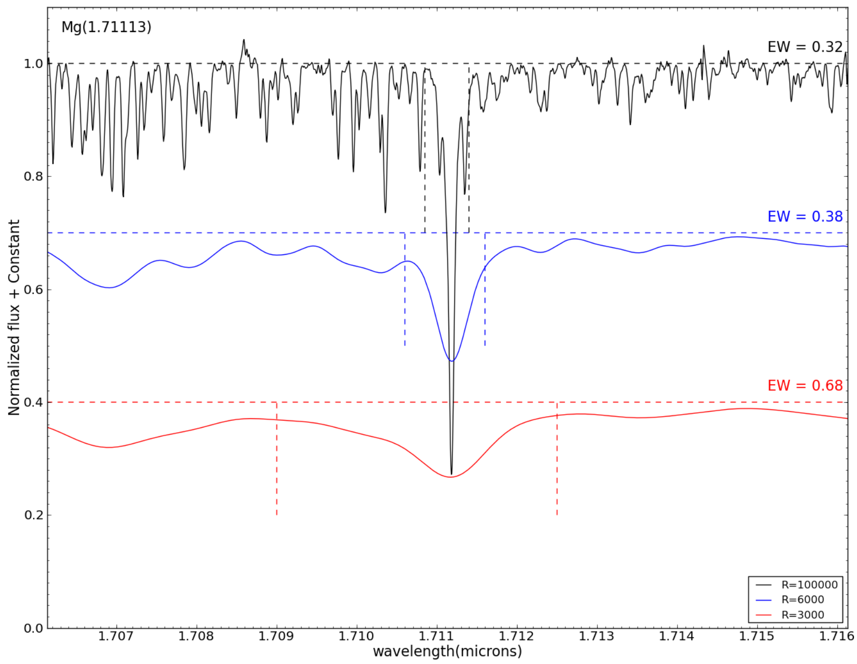

Fig. 9.— Mg (1.71113 μm) line is a single line, and very sensitive to the temperature of giant stars. The wavelength range of EW measurement for R = 100000 and R = 6000 is similar to each other, so the difference of EWs between R = 100000 and R = 6000 is negligible. On the other hand, in the case of R = 3000, it is difficult to define the wavelength range and to measure the EW of this line.

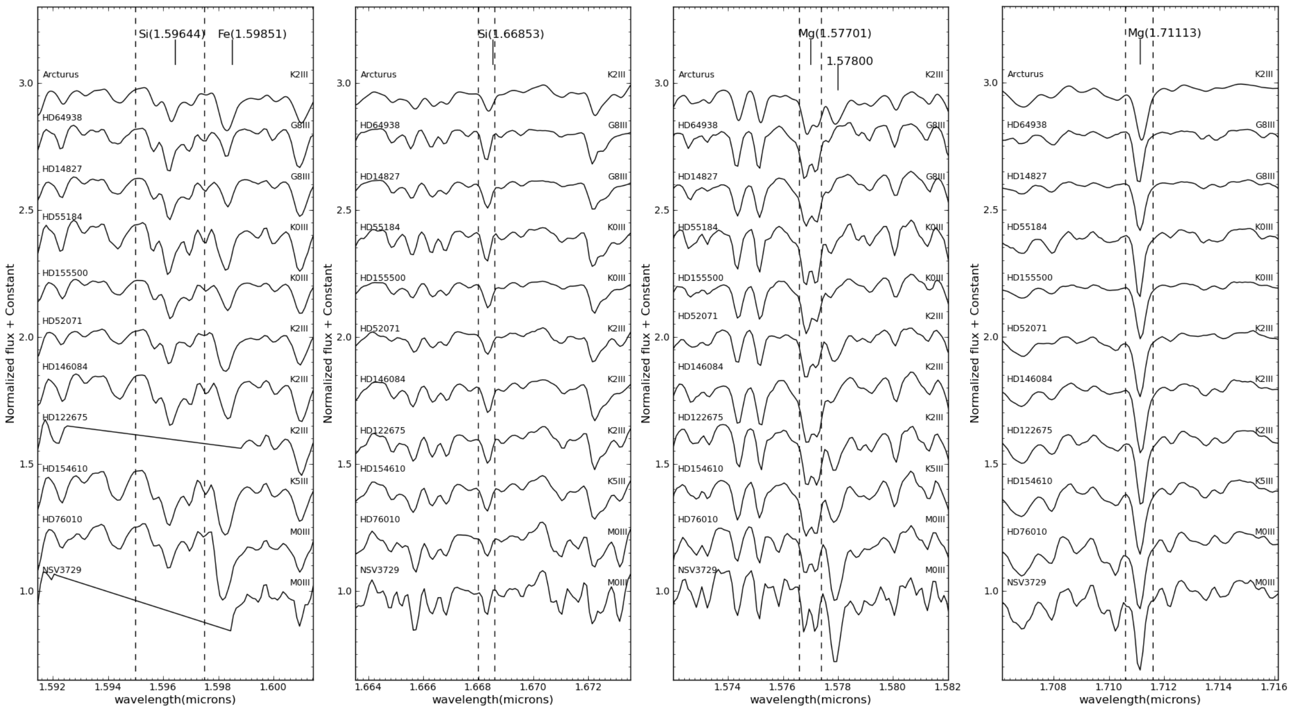

Fig. 10.— The Si (1.59644 μm), Si (1.66853 μm), Mg (1.57701 μm), Mg (1.71113 μm) lines for Arcturus and G-K-M type stars. The top spectrum is from the convoluted one of Arcturus with the same resolution of the other spectra. The dark dash lines show the width range for calculating the EWs. Note that the Si (1.59644 μm) line is contaminated with the strong Fe (1.59851 μm) line, and the Mg (1.57701 μm) line might be also contaminated with the nearby line (1.57800 μm).

Table 4.
Equivalent widths[a]

Object Name	Spectral Type	Teff[b] (K)	Mg[5843] (1.71113 μm)	OH[5920] (1.68909 μm)	H[5948] (1.68111 μm)	Al[5980] (1.67235 μm)	Si[5993] (1.66853 μm)	CO[6019] (1.66147 μm)	CO[6170] (1.62073 μm)	Si[6264] (1.59644 μm)	Mg[6341] (1.57701 μm)
HD64938	G8III	4960	0.26±0.02	0.07±0.01	0.58±0.02	0.23±0.02	0.12±0.02	0.06±0.01	0.31±0.04	0.46±0.02	0.43±0.03
HD148287	G8III	4960	0.27±0.03	0.08±0.01	0.56±0.02	0.21±0.02	0.12±0.02	0.05±0.02	0.29±0.03	0.41±0.02	0.43±0.02
HD55184	K0III	4810	0.33±0.04	0.09±0.01	0.25±0.03	0.25±0.03	0.11±0.03	0.22±0.03	0.63±0.06	0.37±0.03	0.50±0.03
HD155500	K0III	4810	0.32±0.03	0.05±0.01	0.39±0.01	0.20±0.02	0.10±0.02	0.09±0.01	0.39±0.02	0.37±0.02	0.43±0.02
HD52071	K2III	4500	0.39±0.03	0.12±0.01	0.15±0.01	0.18±0.02	0.08±0.02	0.22±0.02	0.75±0.04	0.24±0.02	0.37±0.02
HD146084	K2III	4500	0.42±0.03	0.09±0.01	0.29±0.01	0.24±0.02	0.12±0.02	0.16±0.02	0.60±0.04	0.36±0.02	0.57±0.02
HD122675	K2III	4500	0.41±0.03	···	0.21±0.01	0.19±0.02	0.12±0.01	0.41±0.02	0.97±0.03	···	0.47±0.02
HD154610	K5III	3980	0.42±0.03	0.11±0.01	0.09±0.02	0.24±0.03	0.10±0.02	0.30±0.03	0.98±0.05	0.25±0.02	0.48±0.02
HD76010	M0III	3820	0.48±0.03	0.29±0.01	0.04±0.02	0.18±0.03	0.06±0.01	0.51±0.03	1.39±0.06	0.11±0.03	0.32±0.03
NSV3729	M0III	3820	0.49±0.04	···	0.09±0.02	0.21±0.03	0.09±0.02	0.69±0.04	1.55±0.05	···	0.35±0.04

[a] Values in units of cm^{-1}.
[b] Effective temperature taken from Tokunaga (1998a).

Table 5.
Equivalent widths[a] of Arcturus[b] (K2 III)

Spectral Resolution	Mg[6341] Mg(1.57701 μm)	Mg[5843] Mg(1.71113 μm)
$R = 100000$	0.30±0.02	0.32±0.03
$R = 6000$	0.53±0.04	0.38±0.04
$R = 3000$	1.21±0.07	0.68±0.07

[a] Values in units of cm^{-1}.
[b] Spectra from Hinkle & Wallace (1995).

that the EW of Si (1.59644 μm) line in M98 includes the strong line of Fe (1.59851 μm), which is increasing with decreasing effective temperature, as seen in Fig. 10.

In the case of Si (1.66853 μm), we can see that it has also many nearby lines which show increasing trend of EW with decreasing effective temperature, as shown in Fig. 10. Therefore, it is obvious that the EW trends of Si lines in M98 are affected by nearby lines which are increasing with decreasing effective temperature.

Fig. 12 shows the different EW trends of Mg

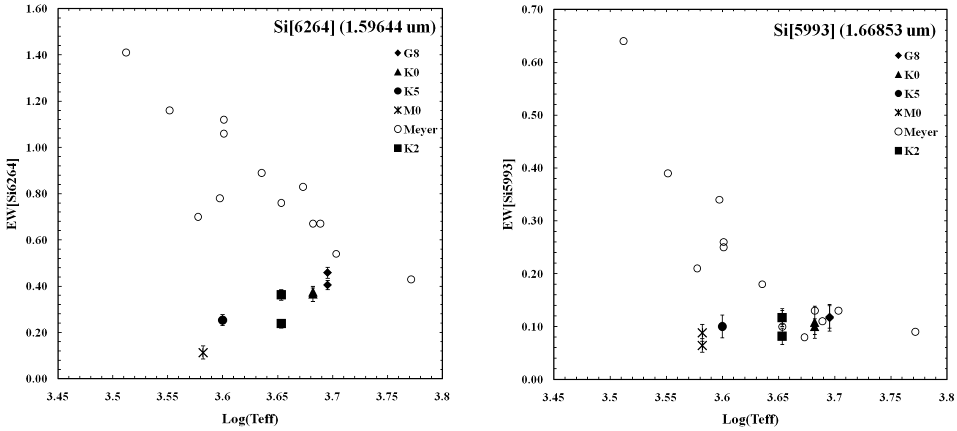

Fig. 11.— EWs of Si (1.59644 μm) and Si (1.66853 μm). Our results are smaller than M98 results because of the different spectral resolution. The trends of Si (1.59644 μm) line are very different compared to M98. The Si (1.59644 μm) line is contaminated with other lines, and in M98 results, they may have used the width range which is too wide and consequently contaminated with other lines including the strong Fe (1.59851 μm) line. This strong Fe line makes our results very different from that of M98.

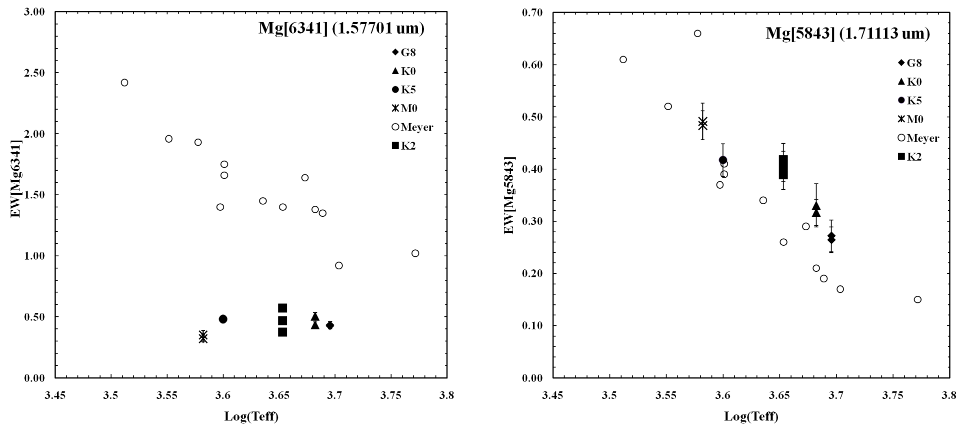

Fig. 12.— EWs of Mg (1.57701 μm) and Mg (1.71113 μm). Mg (1.57701 μm) is contaminated with other lines, but Mg (1.71113 μm) is a single line. Our results are smaller than M98 results because of the different spectral resolution. The width ranges used for calculated EWs in M98 may be wider than ours, and made the results different. This we can be seen in comparison of EWs of two Mg lines of Arcturus spectrum with different resolution. The single Mg (1.71113 μm) line is very sensitive to the effective temperature, and we use this line to estimate effective temperature of late-type stars.

(1.57701 μm) between our result and M98. It is similar to the case of the EW of Si (1.59644 μm) line in M98. In case of Mg (1.57701 μm), M98 calculation might include the strong nearby line of 1.57800 μm which is increasing with decreasing effective temperature.

In Fig. 12, we also find the fact that the Mg (1.71113 μm) line is very sensitive to the temperature of giant stars in G, K, M type, rather than Mg (1.57701 μm) which has been mentioned in M98. The linear fitting of the EWs of Mg line is shown in Fig. 13. Using the EW trend of Mg (1.71113 μm) line for effective temperature, therefore, the relation between effective temperature and EW of Mg line could be obtained by linear fitting. We find the equation to estimate effective temperature from the EW of Mg (1.71113 μm) line as

$$T_{eff} = 6447 \pm 260 - (5230 \pm 672) EW[Mg(5843)] \quad (3)$$

The standard deviation error of the slope in the linear fitting is large because of the low number of stars. This formula can be used to estimate the effective temperature of late-type giant stars (G8 III-M0 III) from EW measurement.

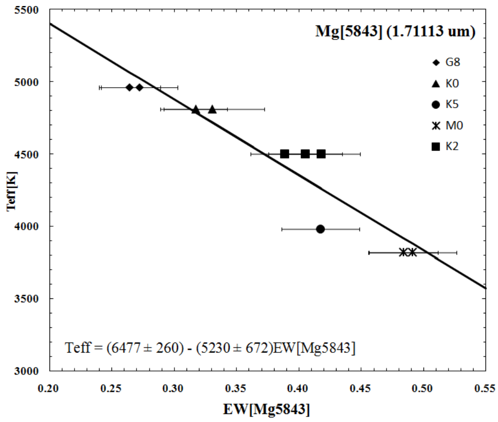

Fig. 13.— Linear fitting of EWs of Mg(1.71113 μm) vs. effective temperature. The error bars indicate the errors of EW for each star that have been calculated from formula (2).

4. SUMMARY AND FUTURE WORKS

We present the method for data analysis of the near-IR medium resolution echelle spectrometer, IRCS, at the SUBARU 8.2m telescope. From the method, we have shown the medium resolution template star spectra of HD64938 and HD148287 (G8 III), HD55184 and HD155500 (K0 III), HD52071, HD146084, and HD122675 (K2 III), HD154610 (K5 III), and HD76010 and NSV3729 (M0 III) in H-band.

We found many prominent molecular and neutral metal features in the template star spectra. We measured the EWs of the features and compare our results to M98 results. Our results with spectral resolution (R = 6000) are more accurate than M98 with spectral resolution (R = 3000). We use the Mg(1.71113 μm) line to estimate approximate temperature for late-type stars.

In this work, the obtained H-band spectra of late-type stellar templates would play important roles for studying relation between active galactic nuclei (AGNs) and their host galaxy properties. The broad absorption $\nu = 3 - 6$ ^{12}CO band head at 1.62073 μm obtained from the spectra is potentially useful for measuring the velocity dispersion in the central region of the QSO host galaxies. The library of the template stellar spectra in ASCII format can be downloaded from the website http://irlab.khu.ac.kr/∼anh/file/StellarData.zip

ACKNOWLEDGMENTS

This work was supported by the National Research Foundation of Korea (NRF) grant funded by the Korean government (MEST), No. 2009-0063616.

REFERENCES

Cutri, R. M., Skrutskie, M. F., Van Dyk, S., et al., 2003, 2MASS All-Sky Catalog of Point Sources, VizieR Online Data Catalog, 2246, 0

Heras, A. M., et al. 2002, Infrared Spectral Classification of Normal Stars, A&A, 394, 539

Hinkle, K., & Wallace, L. 1995, Infrared Atlas of the Arcturus Spectrum, 0.9-5.3 microns, PASP, 107, 1042

Kobayashi, N., et al. 2000, IRCS: Infrared Camera and Spectrograph for the Subaru Telescope, SPIE, 4008, 1056

McConnell, N. J., Ma, C. P., Graham, J. R., Gebhardt, K., Lauer, T. R., Wright, S. A., & Richstone, D. O. 2011, The Black Hole Mass in The Brightest Cluster Galaxy NGC 6086, ApJ, 728, 100

Meyer, M. R., Edwards, S., Hinkle, K. H., & Strom, S. E. 1998, Near-Infrared Classification Spectroscopy: H band Spectra of Fundamental MK Standards, ApJ, 508, 397

Pyo, T. S. 2002, Near Infrared [Fe II] Spectroscopy of Jets and Winds Emanating from Young Stellar Objects, Ph.D. thesis, Tokyo Univ.

Pickles, A. J. 1998, A Stellar Spectral Flux Library: 1150-25000 A, PASP, 110, 863

Ranade, A. C., Ashok, N. M., Singh, H. P., & Gupta, R. 2007, A Near-Infrared Stellar Spectral Library: III. J-band Specrta, BASI

Rayner, J. T., Cushing, M. C., & Vacca, W. D. 2009, The Infrared Telescope Facility (IRTF) Spectral Library: Cool Stars, ApJS, 185, 289

Riffel, R. A., Storchi-Bergmann, T., Winge, C., McGregor, P. J., Beck, T., & Schmitt, H. 2008, Mapping of Molecular Gas inflow towards the Seyfert Nucleus of NGC4051 Using Gemini NIFS, MNRAS, 385, 1129

Rousselot, P., Lidman, C., Moreels, G., & Monnet, G. 2000, Night-sky Spectral Atlas of OH Emission Lines in the Near-Infrared, A&A, 354, 1134

Ryde, N., Edvardsson, B., Gustafsson, B. Eriksson, K., Kaufl, H. U., Siebenmorgen, R., & Smette, A. 2009, Abundances in Bulge Stars from High-Resolution, Near-IR Spectra, A&A, 496, 701

Wallace, L., & Hinkle, K. 1997, Medium- Resolution Spectra of Normal Stars in The K Band, ApJS, 111, 445

Winge, C., Riffel, R. A., & Storchi-Bergmann, T. 2009, The Gemini Spectral Library of Near-IR Late-Type Stellar Templates and Its Application for Velocity Dispersion Measurements, ApJS, 185, 186

Tokunaga, A. 1998a, in Astrophysical Quantities, ed. A. Cox (4th ed.; New York: Springer), in press, 149-153

Tokunaga, A. T., et al. 1998b, Infrared camera and spectrograph for the SUBARU Telescope, SPIE, 3354, 512